

## COMPOSITIONAL TRENDS OF THE GLASS TRANSITION AND CRYSTALLIZATION IN $\text{Te}_{20}\text{Se}_{80-x}\text{Sb}_x$ CHALCOGENIDE GLASSES

A. A. ELABBAR\*

*Physics Department, Taibah University, Madina, Saudi Arabia*

Compositional trend of the glass transition temperature and the effective activation energies of the glass transition and crystallization processes in  $\text{Te}_{20}\text{Se}_{80-x}\text{Sb}_x$  glasses ( $x = 1.5, 3, 4.5, 6, 7.5, 9$  at.%) was investigated by differential scanning calorimetry (DSC) technique. The concept of mean coordination number,  $\langle r \rangle$ , was used to describe the connectivity of the covalent networks of the present samples. The connectivity is enhanced with Antimony as indicated by an increase in  $T_g$  with  $x$ . Two linear regions in the  $T_g(x)$  relationship can be identified with a kink observed at  $x \approx 4.5$  corresponding to  $\langle r \rangle \approx 2.045$ . A striking similarity between the kinetic behavior of glass transition and crystallization processes was found. In both processes, a change in behavior was observed at the same crossover mean coordination number.

(Received October 24, 2014; Accepted December 8, 2014)

*Keywords:* Chalcogenide glasses; DSC; Glass transition; Crystallization, mean coordination number; Topological threshold.

### 1. Introduction

The role of network connectivity of the glassy materials in determining many of their physical properties has been extensively investigated. This growing interest arise from the vital information provided by the relationship between network connectivity and the physical behavior of the glasses which can be used to obtain better understanding of glassy state and can lead to better optimization of glasses for a variety of applications.

The glass network connectivity can be described by the mean coordination number  $\langle r \rangle$  of glassy alloys which according to Mott [1] can be determined using N-8 rule, where N is the number of the outer shell electrons. The mean coordination number can be changed in a controlled manner by varying the composition of the glass. For a covalently bonded alloy  $A_a B_b C_c$ , the mean coordination number is given by

$$\langle r \rangle = \frac{ar_A + br_B + cr_C}{a + b + c} \quad (1)$$

where  $r_A$ ,  $r_B$  and  $r_C$  are the coordination numbers of the constituent atoms. Thus, for  $\text{Te}_{20}\text{Se}_{80-x}\text{Sb}_x$  glasses,  $\langle r \rangle$  is given by

$$\langle r \rangle = \frac{20r_{Te} + (80 - x)r_{Se} + xr_{Sb}}{100} \quad (2)$$

In addition to their outstanding technological applications, chalcogenide glasses represent typical examples of covalently bonded networks which progressively stiffen as their mean coordination number increases.

---

\*Corresponding author. elabbar60@yahoo.com

Considerable amount of research has been devoted to the compositional trends of mechanical and thermal properties of chalcogenide glasses when Phillips and Thorpe [2-4] developed the constraint theory and rigidity percolation to describe the covalent networks of these glasses. Based on these considerations, a phase transition from flexible (or floppy) to rigid phases were predicted at a percolation threshold  $r_c = 2.4$ .

The aim of the present work is to investigate the role played by glass network connectivity on different kinetic parameters of the glass transition and crystallization in  $\text{Te}_{20}\text{Se}_{80-x}\text{Sb}_x$  ( $x = 1.5, 3, 4.5, 6, 7.5, 9$  at.%) chalcogenide glasses. The relationship between  $T_g$  and the mean bond energy is also considered.

## 2. Experimental

The  $\text{Te}_{20}\text{Se}_{80-x}\text{Sb}_x$  chalcogenide glasses were prepared using the standard melt-quench technique. High purity (99.999%) Se, Te and Sb in appropriate atomic weight percentage were weighed and sealed in a quartz ampoule (12 mm diameter) under a vacuum of  $10^{-5}$  Torr. The contents were heated at around 950 K for 24 hours. During the melting process, the tube was frequently shaken to homogenize the resulting alloy. The melt was quenched in ice water to obtain the glassy state. The content of the alloy was checked by Energy Dispersive X-ray (EDX) using the scanning electron microscope (Shimadzu Superscan SSX-550).

Thermal behavior was investigated using Shimadzu DSC-60. The calorimetric sensitivity is  $\pm 10 \mu\text{W}$  and the temperature accuracy is  $\pm 0.1$  K. Typically, 3 mg of sample in powder form was sealed in standard pans and heated at different rates 2,3,4,5,7,10,12,15,17,20 and 25 K/min under dry nitrogen supplied at the rate 35 ml/min. The procedure we followed in these measurements was to cool the samples with one cooling rate and then reheat with many heating rates. To minimize the temperature gradient the samples were well granulated to form uniform fine powder and spread as thinly as possible on the bottom of the sample pan. Temperature and enthalpy calibration was carried out with indium at heating rate 10 K/min ( $T_m = 156.6$  °C.  $\Delta H_m = 28.55$  J/g) as the standard material supplied by Shimadzu.

## 3. Results and discussion

In DSC measurements, the glass transition temperature,  $T_g$ , is identified from the endothermic drop of the DSC signal. The DSC outputs showing the endothermic effect followed by crystallization peak for  $\text{Te}_{20}\text{Se}_{80-x}\text{Sb}_x$  chalcogenide glasses obtained at different compositions ( $x = 1.5$  and 6 %) are shown in Fig. 1. A shift of both  $T_g$  and  $T_p$  (the peak temperature of the crystallization curves) toward higher temperatures is observed. The pronounced endothermic peaks observed for glass transition in Fig. 1 can be attributed to the physical aging. It is interesting to note that the physical aging effect is very similar in both samples as their endothermic peaks have almost the same area.

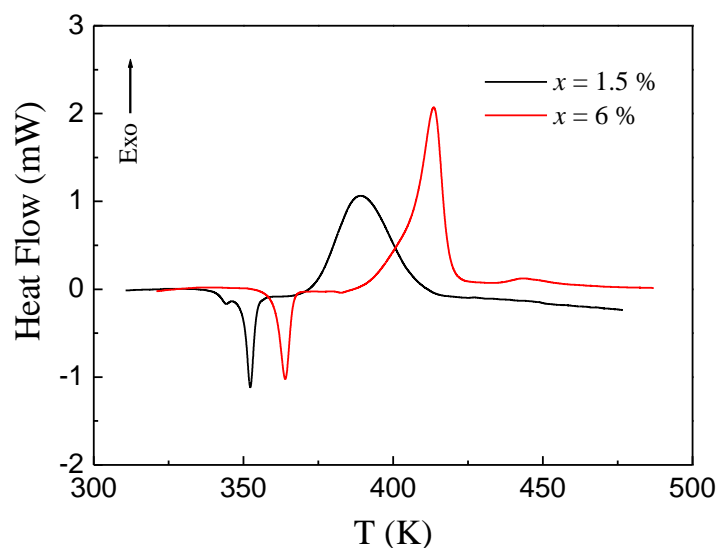


Fig. 1 DSC curves of the  $\text{Te}_{20}\text{Se}_{80-x}\text{Sb}_x$  ( $x = 1.5$  and  $6$ ) chalcogenide glasses at heating rate  $10$  K/min.

The variation of the glass transition temperature,  $T_g$ , is a useful probe for the glass network connectivity. Fig. 2 shows the variation of  $T_g$  with composition,  $x$ , as observed in the DSC measurements of  $\text{Te}_{20}\text{Se}_{80-x}\text{Sb}_x$  glasses. Several important features in the compositional trend of  $T_g$  is evident from Fig. 2.  $T_g$  increases with increasing  $x$ . This behavior indicates that adding Sb atoms into the Te-Se matrix increases the connectivity of the glass network. Two regions of linear dependence of  $T_g(x)$  relationship with a kink at  $x = 4.5$  marking a change in slope are observed. According to Table 1, the change in slope occurs at a quite low value of the mean coordination number ( $\langle r \rangle = 2.045$ ). The change in slope the  $T_g(x)$  trend is a clear indication of a significant change in network connectivity in the  $\text{Te}_{20}\text{Se}_{80-x}\text{Sb}_x$  glasses. This is an additional topological threshold of the glass network that appears at  $\langle r \rangle = 2.045$ , a much lower value than the widely observed rigidity percolation threshold at  $\langle r \rangle = 2.4$ . A similar behavior was observed by Vanitha et al [5] in  $\text{Te}_{20}\text{Se}_{80-x}\text{Sb}_x$  glasses at  $x = 6$ . A crossover in the variation of  $T_g$  with  $x$  in  $\text{Te}_{20}\text{Se}_{80-x}\text{Sb}_x$  glasses was also reported at  $x = 4$  by Sachdev et al [6]. A discontinuity in the photoconductivity was observed at  $x = 4$  in  $\text{Se}_{70}\text{Te}_{30-x}\text{Sb}_x$  glasses by Dwivedi et al [7]. The existence of topological thresholds at low mean coordination numbers were reported by Mikla [8] in  $\text{As}_x\text{Se}_{100-x}$  and Thiruvikraman [9] in  $\text{As}_x\text{S}_{100-x}$  glasses. In the case of  $\text{As}_x\text{Se}_{100-x}$ , a change of structural regime takes place at  $x = 4$ .

The variation of the glass transition temperature with chemical composition (or mean coordination number) was addressed by Micoulaut and Naumis [10]. On the basis of the stochastic agglomeration theory, and considering the modified Gibbs-Di Miazario equation [11],

$$T_g = \frac{T_0}{1 - \beta(\langle r \rangle - 2)} \quad (3)$$

where  $\beta$  is a system dependent parameter, Micoulaut and Naumis [10] derived the following formula for the constant  $\beta$  as:

$$\beta^{-1} = (r_{\text{Te}} - 2)\ln\left(\frac{r_{\text{Te}}}{2}\right) + (r_{\text{Sb}} - 2)\ln\left(\frac{r_{\text{Sb}}}{2}\right) \quad (4)$$

or  $\beta^{-1} = \ln(3/2)$  which gives  $\beta = 0.4$ . Fitting the experimental data ( $T_g$  vs  $\langle r \rangle$ ) to Eq. 3 using  $T_0$  and  $\beta$  as adjustable parameters, we obtain (shown in the inset of Fig. 2) an excellent fit with

$T_0 = 350$  K and  $\beta = 0.6$ . The obtained (experimental) value of  $\beta$  is different from the predicted value according to Eq. 4. However, it is within the range of values (0.3 – 0.7) reported for a variety of chalcogenide glasses [10,11].

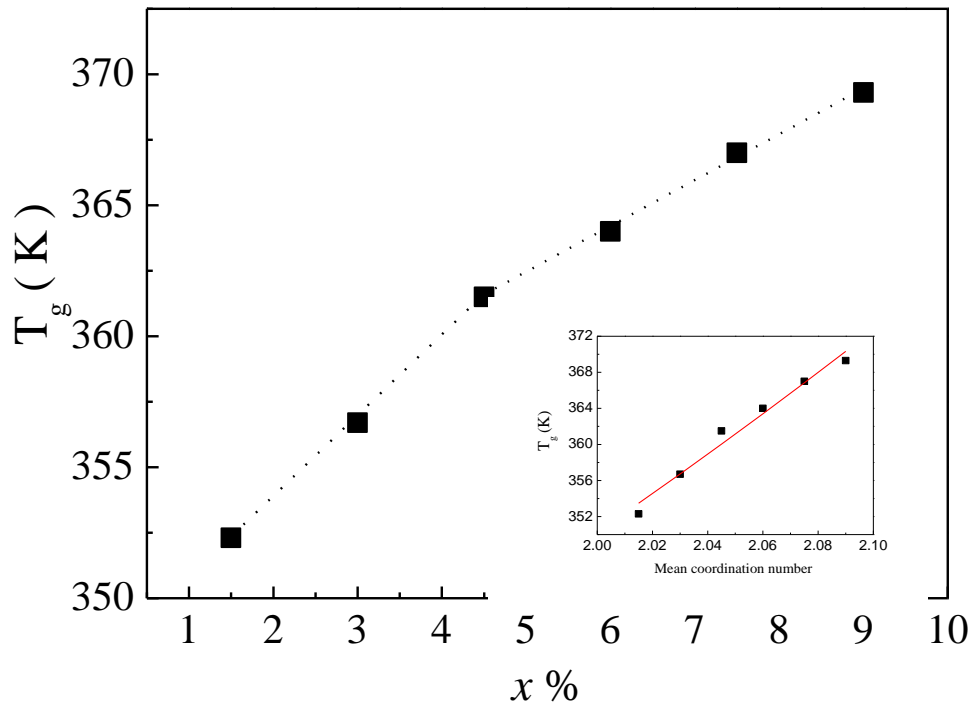


Fig.2 Compositional trend of  $T_g$ . The dotted line in the main panel is a guide for the eye to indicate a change in slope of the  $T_g(x)$  relationship. The inset shows  $T_g$  vs.  $\langle r \rangle$ . The solid line represents the least-squares fitting to Eq. 3.

The change in behavior at  $x \approx 4.5$  is more evident in the compositional trend of  $T_p$ . As can be seen from Fig. 3 that the crystallization temperature  $T_p$  of  $\text{Te}_{20}\text{Se}_{80-x}\text{Sb}_x$  glasses increases with composition  $x$  exhibiting a maximum at  $x \approx 4.5$  (or  $\langle r \rangle \approx 2.045$ ) followed by an initial decrease and finally  $T_p$  becomes almost  $x$ -independent.

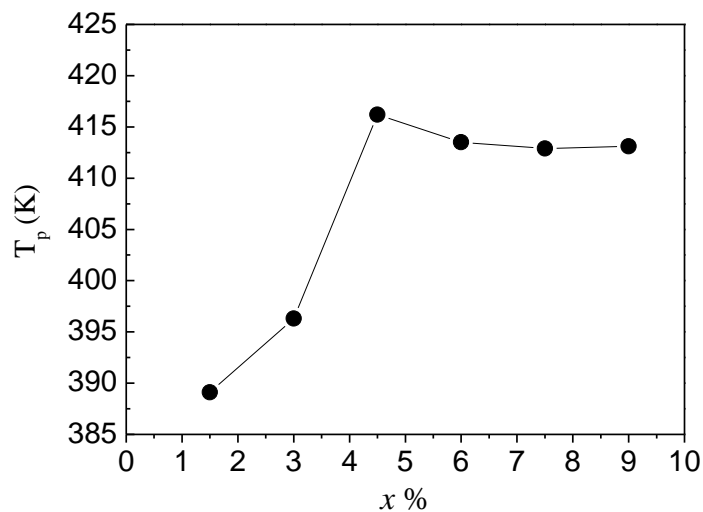


Fig. 3 Compositional trend of the crystallization temperature,  $T_p$ . The maximum value of  $T_p$  occurs at  $x = 4.5$ .

It is well known that  $T_g$  and  $T_p$  both shift to higher temperatures with increasing heating rates. An example of this heating-rate dependence is shown in Fig. 4 for the  $\text{Te}_{20}\text{Se}_{74}\text{Sb}_6$  glass. The heating rate dependence of  $T_g$  and  $T_p$  can be used to estimate the activation energies of glass transition ( $E_g$ ) and crystallization ( $E_c$ ) processes, respectively. Using the Kissinger method, the activation energy for crystallization can be obtained from the following equation [12]:

$$\frac{d \ln(\beta/T_p^2)}{d(1/T_p)} = -\frac{E_c}{R} \quad (5)$$

On basis of the free volume model of glass transition, Ruitenberg [13] showed that the Kissinger method for determining the activation energy for crystallization process can also be used to determine the glass transition activation energy.

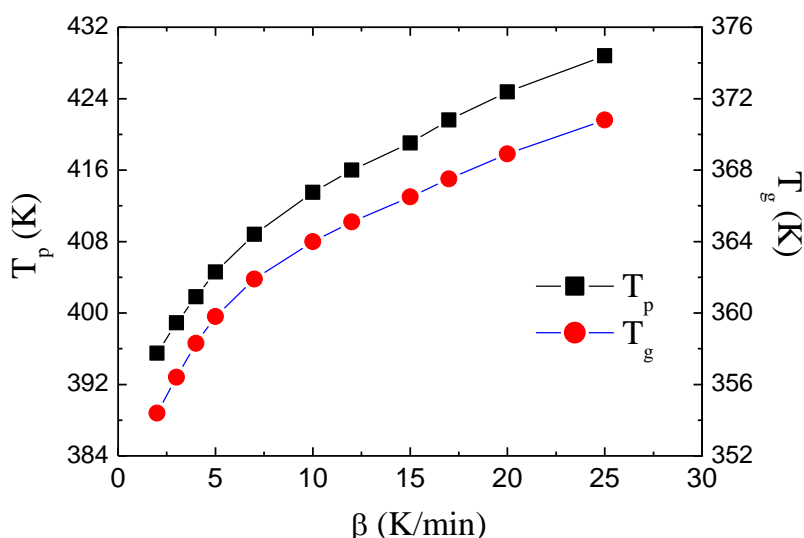


Fig. 4 Heating-rate dependence of the glass transition temperature,  $T_g$ , and crystallization temperature,  $T_p$ .

Therefore, the glass transition activation energy can be obtained using the following equation:

$$\frac{d \ln(\beta/T_g^2)}{d(1/T_g)} = -\frac{E_g}{R} \quad (6)$$

It has been widely reported [14-19] that the values of  $E_g$  obtained using Eq. 6 is very close to values obtained using a method originally suggested by Bartenev and Ritland [20,21] and commonly given in the following form [22]:

$$\frac{d \ln \beta}{d(1/T_g)} = -\frac{E_g}{R} \quad (7)$$

Using Eqs. 5 & 6, the activation energies for crystallization and glass transition at different compositions can be determined by plotting  $\ln(\beta/T_p^2)$  versus  $1/T_p$  and  $\ln(\beta/T_g^2)$  versus  $1/T_g$ , respectively. As can be seen from Fig. 5, the data can be well fitted to straight lines indicating the applicability of Eqs. 6. The compositional trend of the activation energy,  $E_g$ , calculated from the slopes of these straight lines is shown in Figs 6.

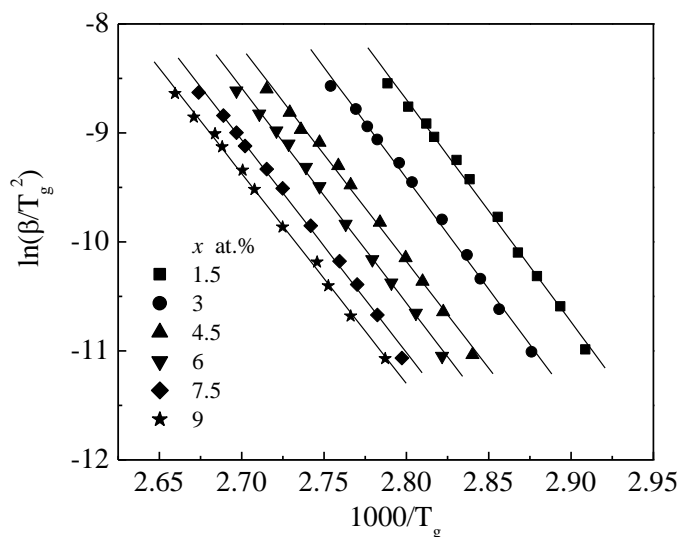


Fig. 5 Kissinger plots for  $\text{Te}_{20}\text{Se}_{80-x}\text{Sb}_x$  glasses. The solid lines are least-squares fitting to Eq. 6.

A similar data analysis was performed to determine  $E_c$  at different compositions. Fig. 7 shows the compositional trend of  $E_c$ . A discontinuity in  $E_g(x)$  graph at  $x \approx 4.5$  is evident in Fig. 6. A more pronounced crossover at about the same compositional threshold is observed in variation of  $E_c$  with  $x$  (Fig. 7). The results of Figs 6 & 7 are further support to the existence of topological threshold at  $x \approx 4.5$  in  $\text{Te}_{20}\text{Se}_{80-x}\text{Sb}_x$  glasses.

A possible observed change in slope in  $T_g(x)$  dependence as well as the crossover behavior observed in the compositional trends in  $T_g$ ,  $E_g$ ,  $E_c$  can be attributed to a topological transition in the glass network at  $x \approx 4.5$ . This is similar to the previously reported transition in Te-Se-Sb and other chalcogenide glasses [5-9]. Such a topological transition is a signature of a transformation of dimensionality,  $D$ , of the glass network commonly observed in low coordinated chalcogenide glasses. As pointed out by Mikla [8], it is possible that cross-linking of the Se and Te-Se chains caused by the 3 coordinated Sb atoms transforms the network from the ring-chain-like structure ( $D \leq 1$ ) to a chainlike ( $D \geq 1$ ) structure.

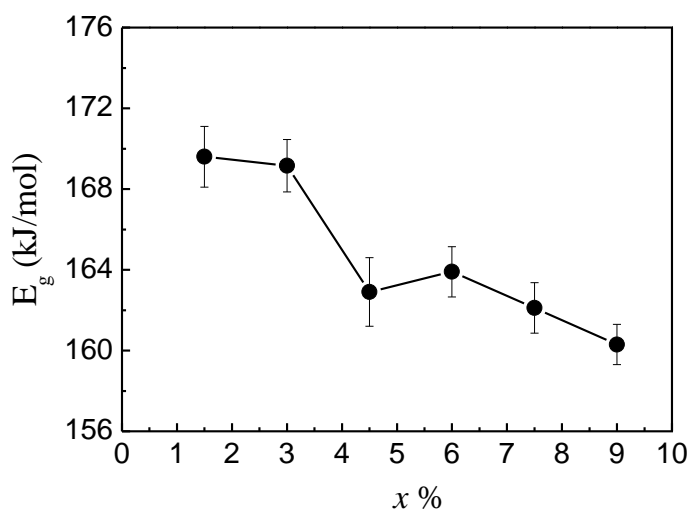


Fig. 6 Compositional trend of the activation energy of the glass transition. The solid line is a guide to the eye.

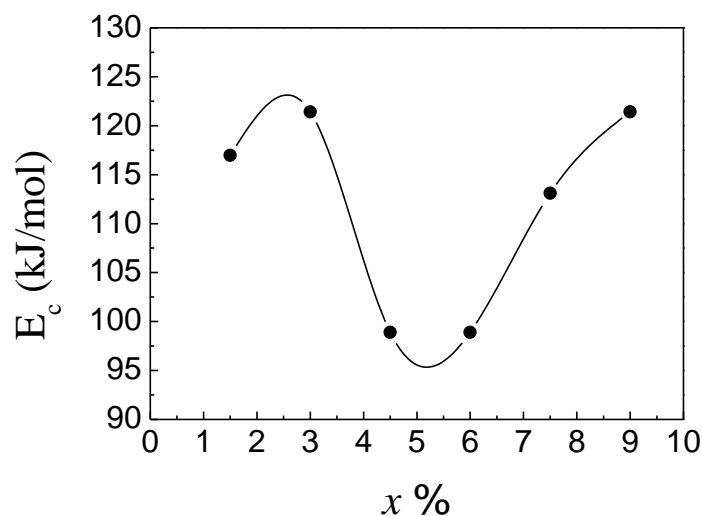


Fig. 7 Compositional trend of the activation energy of crystallization process. The solid line is a guide to the eye.

As pointed out by Tichy and Ticha [23], the compositional trend of  $T_g$  is not only related to the connectivity of the glass network but it can also be related to the mean bond energy between the atoms of the network. The mean bond energy  $\langle E \rangle$  for  $\text{Te}_{20}\text{Se}_{80-x}\text{Sb}_x$  glasses can be written as:

$$\langle E \rangle = E_c + E_{rm} \quad (8)$$

where  $E_c$  is the average heteropolar bond energy and is defined by,

$$E_c = \frac{20r_{\text{Te}}E_{\text{Te-se}} + xr_{\text{Sb}}E_{\text{Sb-se}}}{100} \quad (9)$$

and the average bond energy per atom of the remaining matrix  $E_{rm}$  is given by:

$$E_{rm} = \frac{r_{\text{Se}} \left( \frac{1}{2} \langle r \rangle - \frac{1}{100} [20r_{\text{Te}} + xr_{\text{Sb}}] \right) E_{\text{Se-se}}}{\langle r \rangle} \quad (10)$$

$E_{\text{Te-Se}}$ ,  $E_{\text{Sb-Se}}$  and  $E_{\text{Se-Se}}$  are Te-Se, Sb-Se and Se-Se bond energies, respectively. According to Pauling [24], the values of the bond energies  $E_{\text{Te-Se}}$ ,  $E_{\text{Sb-Se}}$  and  $E_{\text{Se-Se}}$  are 1.86, 1.86 and 1.9 eV, respectively. Thus, using Eqs 8-10, the mean bond energy can be determined at different compositions (or at different  $\langle r \rangle$ ). The calculated values of  $\langle E \rangle$  are given in Table 1.

Table 1. Composition, mean coordination number and mean bond energy of the  $\text{Te}_{20}\text{Se}_{80-x}\text{Sb}_x$  calcogenide glasses.

x (at.%)	$\langle r \rangle$	$\langle E \rangle$ (eV)
1.5	2.015	1.889
3	2.030	1.894
4.5	2.045	1.901
6	2.060	1.909
7.5	2.075	1.917
9	2.090	1.928

An empirical relationship describing the variation of  $T_g$  with the mean bond energy of the glass network was suggested by Tichy and Ticha [23]:

$$T_g = 311(\langle E \rangle - 0.9) \quad (11)$$

In order to test the validity of Tichy and Ticha equation,  $T_g$  is plotted against  $\langle E \rangle - 0.9$  in Fig. 8. A reasonable expression representing the data in Fig. 8 is:

$$T_g = 360(\langle E \rangle - 0.9) \quad (12)$$

which does not agree with Tichy and Ticha equation (Eq. 11). The entire data can not be described by a single expression of the form of Tichy and Ticha equation due the change in slope at  $x = 4.5$  topological threshold.

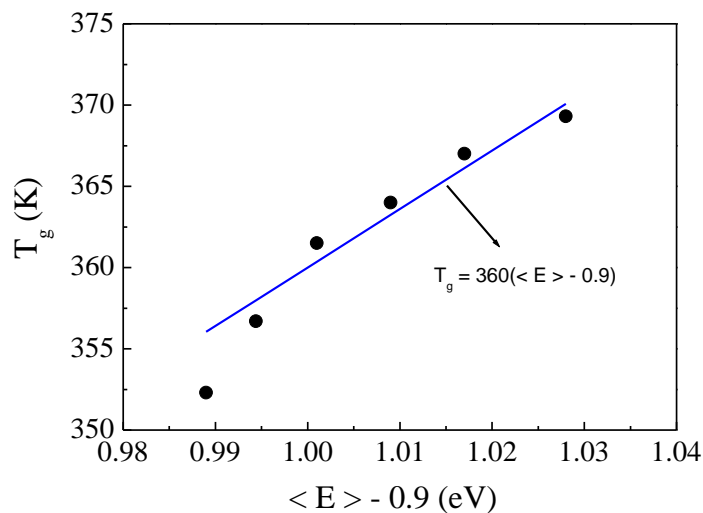


Fig.8. Glass transition temperature variation as a function of  $\langle E \rangle - 0.9$ .

#### 4. Conclusions

Experimental evidence for changes in bonding topology in  $\text{Te}_{20}\text{Se}_{80-x}\text{Sb}_x$  chalcogenide glasses is reported. The compositional trends in various physical parameters indicate a topological threshold in the glass network structure at  $x = 4.5$ . It is suggested that topology threshold arise when the glass undergoes a transition from a structure dominated ringlike segments to a structure with appreciable chains consisting of Se and Te.

#### References

- [1] N.F. Mott, Philos. Mag. **19**, 835 (1969).
- [2] J.C. Phillips, J. Non-Crys. Solids **34**, 153 (1979).
- [3] M.F. Thorpe, J. Non-Crys. Solids **57**, 355 (1983).
- [4] J.C. Phillips, M.F. Thorpe, Solid State Comm. **53** 699 (1985).
- [5] M.K. Vanitha, M.V. Hanumantha Rao, S. Asokan, K. Ramesh, J. Phys. Chem. Solids **74**, 804 (2013).
- [6] V. K. Sachdev, Sandeep Kohli, P. C. Mathur, and R. M. Mehra, Phys. Stat. Sol. (a) **155**, 461 (1996).
- [7] P. K. Dwivedi, S. K. Srivestava and A. Kumar, IL Nuovo Cimento **15D**, 1149 (1993).
- [8] V.I. Mikla, J. Phys : Condens. Mater. **9** 9209 (1997).



- [9] P.K. Thiruvikraman, Bull. Mater. Sci **29**, 371 (2006).
- [10] M. Micoulaut, G.G. Naumis, Europhys. Lett. **47**, 568 (1999).
- [11] A.N. Sreeram, D.R. Swiler, A.K. Varshneya, J. Non-Crys. Solids **127**, 287 (1991).
- [12] H.G. Kissinger, Anal. Chem. **29**, 1702 (1957).
- [13] G. Ruitenber, Thermochem. Acta **404**, 207 (2003).
- [14] A.A. Elabbar, Physica B **403**, 4328 (2008).
- [15] A.A Elabbar, J. Alloys & Compounds **476**, 125 (2009).
- [16] N. Mehta, K. Singh, A. Kumar, Physica B **404**, 1835 (2009).
- [17] N. Mehta, A. Kumar, J. Non-Crys. Solids **358**, 2783 (2012).
- [18] N. Mehta, R.K. Shukla, A. Kumar, Chalcogenide Lett. **1**, 131 (2004).
- [19] O. A. Lafi, M.M.A. Imran, M.K. Abdullah, Physica B **395**, 69 (2007).
- [20] G. Bartenev, Dokl. Akad. Nauk. SSSR **76**, 227 (1951).
- [21] H. Ritland, J Amer Ceram Soc **37**, 370 (1954).
- [22] C.T. Moynihan, A.J. Easteal, J Wilder, and J. Tucker, J. Phys. Chem. **78**, 2673 (1974).
- [23] L. Tichy, H. Ticha, J. Non-Crys. Solids **141-146**, 185 (1995).
- [24] L. Pauling, The nature of the chemical bond, Cornel University press, Ithaca, USA, 1948.